K^-p Interactions at 1.15 BeV/c

WILLIAM GRAZIANO AND STANLEY G. WOJCICKI
Lawrence Radiation Laboratory, University of California, Berkeley, California

(Received July 5, 1962)

This paper contains the conclusion of the systematic study of K^-p interactions in the Lawrence Radiation Laboratory's 15-in. hydrogen bubble chamber at 1.15 BeV/c. In particular, we report on the elastic and charge-exchange scattering, K^*N production, and $\Sigma\pi$ reactions. The procedure used in scanning, measuring, and computer analysis is described in detail. The similarity of total as well as differential cross sections for the three $\Sigma\pi$ charge states suggests predominant production from the $T=0$ state for this channel. The angular distributions for the $\Sigma\pi$ reactions, as well as the elastic and charge-exchange scattering, indicate that partial waves as high as $F_{5/2}$ must be involved. The analysis of the $K^-p\pi^0$ reactions substantiates the earlier preliminary result of isotopic spin 1/2 for the K^* resonance. The angular distributions and correlations in the $K^-p\pi^0$ and $K^-\pi^+n$ reactions support the conclusion, derived from the previous study of our $\bar{K}^0p\pi^-$ events, that the K^* spin is 0 or 1. A summary of cross sections for all the reactions studied in the experiment is given.

I. INTRODUCTION

DURING the fall of 1958, the Lawrence Radiation Laboratory's 15-in. hydrogen bubble chamber was exposed to a separated beam of 1.15-BeV/c K^- mesons. A systematic study was undertaken of the interactions produced by the approximately 100 000 K^- mesons that entered the bubble chamber. Partial results of this study are reported elsewhere.[1–4] In this paper, we present data for the following reactions:

$$\begin{aligned} K^-+p &\to KN \\ &\to KN\pi \\ &\to \Sigma\pi \\ &\to \Lambda\pi. \end{aligned}$$

In Sec. II we summarize the K^- beam and discuss the scanning, measuring, and kinematical analysis of our bubble-chamber events. We also describe there briefly the PANG, KICK, and EXAMIN system used in this experiment.

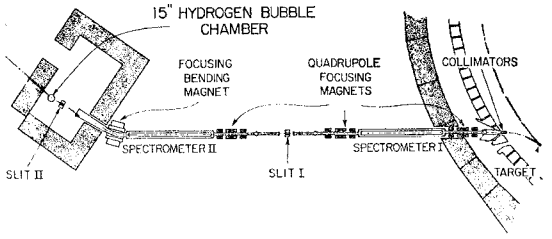

FIG. 1. Schematic drawing of the K^- beam used in this experiment.

The method used in resolving the ambiguities between the different reactions is discussed in Sec. III. This section also describes the corrections that had to be applied to the data to remove the experimental biases.

Section IV summarizes the results of the experiment. In addition to a summary of the cross sections for the K^-p reactions at 1.15 BeV/c, we present the angular distributions for the KN, $\Sigma\pi$, and $\Lambda\pi$ final states. The least-squares fits to power series in $\cos\theta$ for the KN and $\Sigma\pi$ reactions are presented in a table form. Finally, the data on $KN\pi$ events is analyzed in terms of K^*N production.

II. EXPERIMENTAL PROCEDURE

A. K^- Beam

The K^- beam used in this experiment has been described in detail elsewhere[5]; thus, we will summarize only some of its more important characteristics. A schematic drawing of the beam is shown in Fig. 1. The beam was designed to accept negatively charged particles from the Bevatron in the momentum interval from 1155 to 1185 MeV/c; the momentum of the accepted particles was reduced by approximately 20 MeV/c because of ionization loss in the walls of the chamber. Two stages of electrostatic separation were used to separate the K^- mesons from the other particles in the beam.

A preliminary analysis of the ratio of π^- to K^- mesons was made by searching for incident tracks that interacted in the bubble chamber and which had a δ ray with energy greater than 5.83 MeV. These tracks must be π^- mesons, since the maximum δ-ray energy that a 1.15-BeV/c K^- meson can produce, is 5.83 MeV. The results were that the ratio of π^- to K^- was either $50\pm18\%$ or $8\pm11\%$, depending on the adjustment of the spectrometers.[5] The lower-pion contamination could be obtained by a small reduction in the K^--meson flux.

[1] L. W. Alvarez, P. Eberhard, M. L. Good, W. Graziano, H. K. Ticho, and S. G. Wojcicki, Phys. Rev. Letters **2**, 215 (1959).
[2] M. H. Alston, L. W. Alvarez, P. Eberhard, M. L. Good, W. Graziano, H. K. Ticho, and S. Wojcicki, Phys. Rev. Letters **5**, 520 (1960).
[3] M. H. Alston, L. W. Alvarez, P. Eberhard, M. L. Good, W. Graziano, H. K. Ticho, and S. Wojcicki, Phys. Rev. Letters **6**, 300 (1961).
[4] M. H. Alston, L. W. Alvarez, P. Eberhard, M. L. Good, W. Graziano, H. K. Ticho, and S. Wojcicki, Phys. Rev. Letters **6**, 698 (1961).
[5] P. Eberhard, M. L. Good, and H. K. Ticho, Rev. Sci. Instr. **31**, 1054 (1960).

A more accurate estimate of these ratios will be given in Sec. III.

To determine the collimation of the K^- mesons in the beam, we analyzed our τ-decay events. In approximately 93% of these events, the direction of the incident K^- meson was within ± 2.4 deg in azimuth and ± 2.4 deg in dip of a certain fixed direction in space (approximately the average direction of our τ mesons). Therefore, by requiring that the interacting track be within ± 2.4 deg in azimuth and dip of this direction, we were able to reduce the number of events due to π^- and K^- mesons that had scattered in the beam.

The average momentum and momentum spread of the K^- mesons was determined by studying our $K_{\mu 2}$ decays in which the muon stopped. Because the direction and range of a particle can be measured very accurately in a bubble chamber, we can calculate the momentum of the incident K^- meson with an error of only about 5 MeV/c. Furthermore, this method is independent of the magnetic field and thus provides a check on the value of the field used. We had 46 decays in which a muon stopped; three of these did not satisfy our angle criterion for beam tracks. The average momentum for the remaining 43 decays was 1150 ± 3 MeV/c, and the spread was ± 20 MeV/c after unfolding experimental errors.

B. Processing Data

Approximately 75 000 bubble-chamber pictures were taken during the experiment. Each picture was scanned twice for incident tracks that interacted or decayed. The purposes of the second scan were to find events missed on the first scan and to estimate the number of events that were missed on both scans. Since it is difficult to determine on the scanning table if the incident track of an event would satisfy our angle criterion, we retained all interactions and decays in which the incident particle was within approximately ± 5.0 deg in azimuth and dip of the beam direction. The remaining nonbeam events were eliminated after the events were measured. Also, the events were examined by the scanner to determine whether they were within a specified fiducial volume, defined by using the fiducial marks on the top glass of the chamber as reference points. Events outside of this volume are usually difficult to analyze and were therefore rejected. The scanning efficiencies for the events within this volume will be discussed in Sec. III.

Unfortunately, at this momentum the exact reaction cannot be identified merely by visual inspection of an event. Kinematical analysis is necessary for all possible physical interpretations before the correct one can be determined. Thus, during the scanning, no effort was made to identify the reaction. Instead, each event was placed according to its topology into one of eight classifications, called event types. Some of these event types are illustrated in Figs. 2 and 3.

From the four stereo bubble-chamber pictures of an interaction, we selected, for each track of an event, the two views that would give the most accurate spatial reconstruction of the track. A projection microscope, called Franckenstein, was used to obtain the film coordinates of several points on each track in the two views selected.[6]

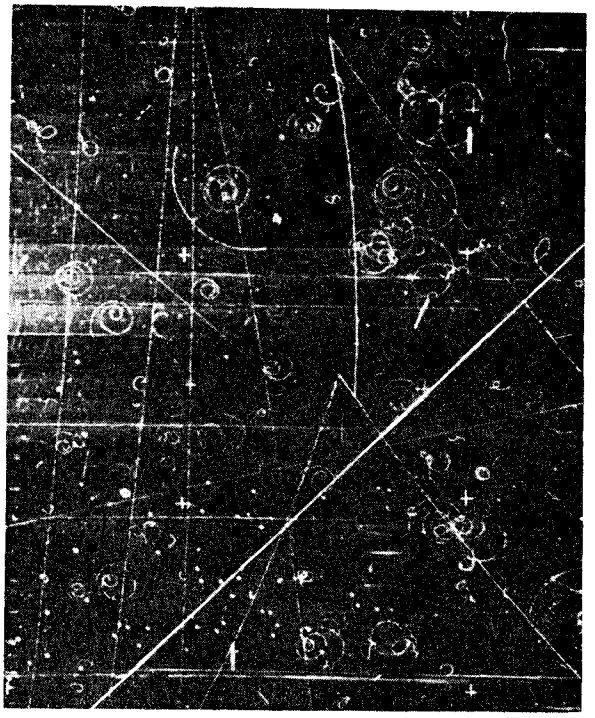

FIG. 2. An example of the reaction:

$$K^- + p \rightarrow K^- + \pi^+ + n,$$
$$K^- + p \rightarrow \Sigma^- + \pi^+ \searrow \pi^- + n.$$

PANG, a program for the IBM 704, utilized these film coordinates to reconstruct each of the tracks in space.[7] Using the event type of the interaction, PANG assigned

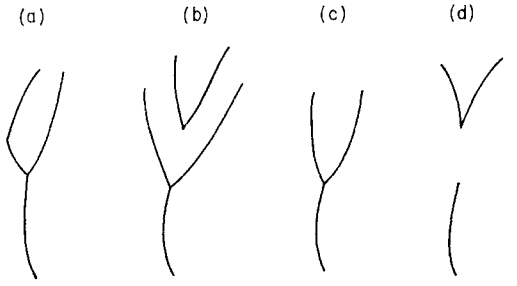

FIG. 3. Illustrations of (a) $\Sigma\pi$, (b) V^0 two-prong, (c) two-prong, and (d) V^0 zero-prong event types.

[6] This microscope was designed by and constructed under the direction of Jack V. Franck at this Laboratory.

[7] William Humphrey, A Description of the PANG Program, Alvarez Group Memo 111, September 18, 1959, and Memo 115, October 25, 1959 (unpublished); Arthur H. Rosenfeld in *Proceedings of the International Conference on High-Energy Accelerators and Instrumentation, CERN, 1959* (CERN, Geneva, 1959).

masses to the particles that produced the tracks. The momentum and space angles, along with their errors, were then calculated for each particle.

Another program, KICK,[8] used the data provided by PANG on a given event to perform a least-squares fit to each of the possible interpretations for this event. It used the four energy-momentum conservation equations as the constraints. For each hypothesis, KICK calculated the χ^2, the fitted momenta and angles for the particles, and the errors on the fitted data. If the incident particle in a given hypothesis was a K^- meson, then KICK would average the momentum obtained from PANG with 1150 ± 20 MeV/c before it performed the fit. This was done because the error on the measured momentum of a 1-BeV/c particle is frequently quite large. A given interpretation was rejected if its χ^2 value corresponded to a probability of less than 1%.

A program named EXAMIN performed calculations on the fitted data from KICK. Since the calculations performed by EXAMIN depend upon the event type, we will discuss them in the section on data analysis.

C. The K^- Pathlength

The path length for the K^- mesons which satisfied our beam criteria was calculated from the number of observed K^- decays. A correction was applied to allow for small-angle decays and because scanning efficiency was less than 100%. The total path length in the entire film sample was such that one observed event corresponded to 12.2 μb. In the restricted film sample for which the ratio of π^- to K^- was 8 ± 11%, one event corresponded to 30.3 μb. Errors associated with the above two cross sections are not given because they are insignificant compared to the errors associated with the numbers of interactions.

III. ANALYSIS OF DATA

A. $K^-+p\rightarrow\Sigma^\pm+\pi^\mp$

Events produced by the reactions $K^-+p\rightarrow\Sigma^\pm+\pi^\mp$ are indistinguishable topologically from $\Sigma^\pm+\pi^\mp+n\pi^0$ ($n=1, 2$) events. Fortunately, the kinematics for these reactions are sufficiently different so that the unambiguous isolation of the two-body events is relatively straightforward. Of the 171 events that fit the $\Sigma\pi$ hypothesis, only 19 also gave a satisfactory fit to a $\Sigma2\pi$ interpretation. Furthermore, the χ^2 distribution for these 19 events when fitted to the $\Sigma\pi$ hypothesis agrees with the expected distribution, whereas the χ^2 distribution when the 19 events are fitted to $\Sigma2\pi$ interpretations is much broader than the expected distribution. This and the improbability that an actual $\Sigma2\pi$ event would fit a $\Sigma\pi$ interpretation lead us to believe that almost all of these 19 events are $\Sigma\pi$ events; we consider them as such in the following analysis.

[8] A. H. Rosenfeld and J. N. Snyder, Rev. Sci. Instr. 33, 181 (1962); J. P. Berge, F. T. Solmitz, and H. Taft, Rev. Sci. Instr. 32, 538 (1961).

For the charged Σ events we first fitted the Σ-decay vertex by using the PANG data on the Σ track and on its charged decay product. Subsequently, the fitted variables of the Σ track were transformed from the decay to the production vertex. The event was then fitted to the $\Sigma\pi$ and $\Sigma2\pi$ hypothesis. Unfortunately, in most of the events the Σ track was so short that its momentum from curvature was unreliable. For these events we were only able to calculate the momentum of the Σ. This calculation frequently resulted in a twofold ambiguity, corresponding to forward or backward center-of-momentum (c.m.) decay (fourfold for Σ^+ events because of the additional protonic decay mode). Thus, for these events, several production fits had to be performed—one for each Σ momentum. Fortunately, the production kinematics are sufficiently constrained so that the ambiguity in the Σ momentum is always resolvable.

In obtaining the angular distributions for the $\Sigma\pi$ reactions, we have to consider the following biases:

1. The scanning efficiency for $\Sigma^\pm\pi^\mp$ events depends upon the angle that the Σ makes with its charged decay product. This is especially serious for forward-produced hyperons which decay via the protonic mode, since the decay angle in the laboratory (lab) system is always less than 9.5 deg for these events. Furthermore, in a protonic decay, one generally does not see a sudden change in ionization, as in a low-energy $\Sigma^\pm\rightarrow n+\pi^\pm$ decay.

2. Events with short Σ tracks tend to be misclassified as two-prong reactions more often than do events with longer Σ tracks. This is a bias against Σ hyperons which are produced in the backward direction. This would be a serious bias if not corrected, since the probability that a backward-produced Σ would decay in the first millimeter is about 30%.

3. At this energy the escape probability becomes significant, since a forward-produced Σ hyperon would have a mean path length of about 6 cm, a relatively large distance in a 15-in. bubble chamber.

To obtain a bias-free distribution we imposed the following requirements on all events:

(1) The projected decay angle between the Σ and its decay product must be more then 10 deg in at least one of the four views.

(2) The Σ track must be at least 4 mm long in space.

(3) The Σ must be produced and decay inside a specified fiducial volume.

The scanning efficiency for the events that satisfied these three requirements is such that it is unlikely that any events were missed in both scans.

All of the $\Sigma\pi$ events were processed through our EXAMIN program, which checked to see that each of these conditions was satisfied (the events that did not satisfy these requirements were rejected). The program also computed the probability that a Σ emitted at the observed angle θ with the observed momentum P would

meet these three requirements. This probability is given by

$$P_{\text{det}}=(P_3-P_2)P_1,$$

where P_3 is the probability of decay within the fiducial volume, P_2 is the probability of decay in the first 4 mm, and P_1 is the probability that the projected decay angle will be greater than 10 deg in at least one of the four views. Each event was then weighted by $1/P_{\text{det}}$.

This method of treating the biases is not satisfactory if physical states with a very low probability of detection are present. Unfortunately, the forward-produced Σ hyperons that decay via the protonic mode ordinarily have a projected decay angle smaller than 10 deg. Therefore, the probability that these Σ^+ events meet the first criterion is almost zero. For this reason, only the events in which the Σ^+ decayed via the pionic mode were used for the forward part of the angular-distribution histogram; the weight for each of these events was multiplied by 2 to take into account the protonic decays (the rates of the two decay modes are experimentally known to be equal). After removal of the forward-produced Σ^+ hyperons that decay via the protonic mode, our method of correcting the biases becomes quite satisfactory (the weights for the events range from about 1.2 to 2.5).

The angular-distribution histograms for the $\Sigma^+\pi^-$ and $\Sigma^-\pi^+$ reactions are shown in Fig. 4. The ordinate represents the sum of the weights for each interval.

To obtain the polarizations of the charged Σ hyperons, we used all of the $\Sigma^\pm\pi^\mp$ events that were found. The above-mentioned scanning biases do not affect the calculation of the polarizations, since the "up" and "down" events are effected equally by these biases. Table I shows that polarization results for the $\Sigma^\pm\pi^\mp$ reactions.

We use the following sign convention. The decay distribution of a spin-1/2 particle in its own rest frame is given by

$$I(\theta)=(1+\alpha P\cos\theta)/2.$$

Here $\cos\theta$ is defined as

$$\cos\theta=\frac{\mathbf{P}_N\cdot(\mathbf{P}_K\times\mathbf{P}_Y)}{p_N|\mathbf{P}_K\times\mathbf{P}_Y|},$$

where $\mathbf{P}_K$, $\mathbf{P}_Y$, $\mathbf{P}_N$ are momenta of the incident K^-, the Σ hyperon, and the decay nucleon, respectively, in either the laboratory or K^-p c.m. system, and p_N is the magnitude of the momentum of the nucleon in the hyperon rest frame.

TABLE I. Observed values of $\alpha\bar{P}$.

Production channel	Decay mode of the hyperon	$\alpha\bar{P}$
$K^-+p\to\Sigma^++\pi^-$	$\Sigma^+\to\pi^++n$	-0.15 ± 0.27
$\to\Sigma^++\pi^-$	$\Sigma^+\to p+\pi^0$	-1.02 ± 0.23
$\to\Sigma^-+\pi^+$	$\Sigma^-\to\pi^-+n$	0.20 ± 0.20
$\to\Lambda+\pi^0$	$\Lambda\to p+\pi^-$	0.09 ± 0.20
$\to\Sigma^0+\pi^0$, $\Sigma^0\to\Lambda+\gamma$	$\Lambda\to p+\pi^-$	0.25 ± 0.26
$\to\Lambda+a\pi^0$ $\}a\geq2$	$\Lambda\to p+\pi^-$	0.12 ± 0.26
$\to\Sigma^0+a\pi^0$, $\Sigma^0\to\Lambda+\gamma$ $\}$		

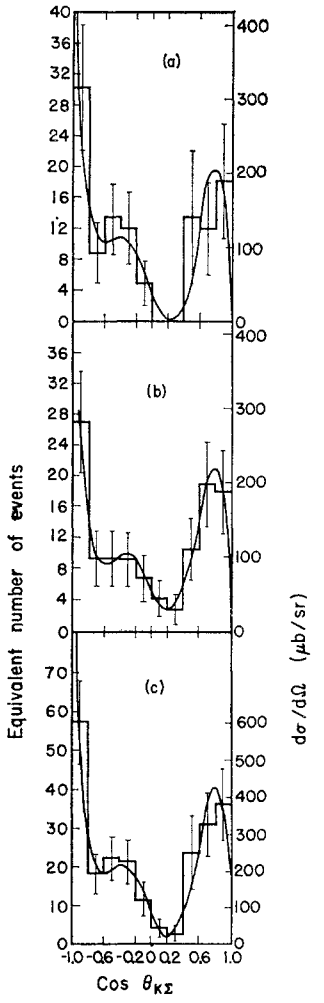

FIG. 4. Angular distribution of $\Sigma^\pm$ in the K^-p c.m. system for the reactions (a) $K^-+p\to\Sigma^++\pi^-$, (b) $K^-+p\to\Sigma^-+\pi^+$, and (c) for both reactions combined. The superimposed curves represent the least-squares fit of the data to the power series in $\cos\theta$ up to $\cos^5\theta$.

B. V^0 Zero-Prong Events

We discuss next the single-V events found in our film. Topologically, they consist of a disappearance of a beam track (0 prong) associated with a V (Fig. 3). They can be due to the following reactions;

$$K^-+p\to\bar{K}^0+n, \quad (1)$$
$$\to\bar{K}^0+n+\pi^0, \quad (2)$$
$$\to\bar{K}^0+n+2\pi^0, \quad (3)$$
$$\to\Lambda+\pi^0, \quad (4)$$
$$\to\Sigma^0+\pi^0, \quad (5)$$
$$\to\Lambda+a\pi^0, \quad (6)$$
$$\to\Sigma^0+a\pi^0. \quad (7)$$

$a\geq2$

The events can be separated relatively easily into one of two groups: one in which the V is a $\bar{K}^0$ decay or one in which the V is a Λ decay. Decay and production

kinematics, along with the ionization of the positive track were used to obtain this separation.

To correct for the bias due to the V's escaping from the chamber before decaying, as well as the immediate decay of the V (the latter would result in misclassification of the event as two-prong), we require that all accepted V's decay inside the specified fiducial volume and that they travel at least 4 mm before decaying. Then, just as for charged Σ's, all events satsifying these criteria are weighted by the inverse of their probability of detection. The scanning efficiency for the events that meet the above two criteria is approximately 100%.

The procedure followed in classifying the $\bar{K}^0$ events was as follows. An event was given a $\bar{K}^0 n$ interpretation if it gave a satisfactory χ^2 to this hypothesis. (The $\bar{K}^0 n$ and $\Lambda\pi^0$ hypothesis are the only ones constrained enough so that a kinematical fit can be made.) It was classified as a $\bar{K}^0 n\pi^0$ event if the invariant mass of the missing neutrals exceeded the mass of the neutron and a π^0. The momentum of the $\bar{K}^0$ obtained by fitting its decay is known to such a high precision that there was no overlap due to measurement errors between the above two reactions. We have assumed that there were no $\bar{K}^0 n\pi^0\pi^0$ events, since no $\bar{K}^0 p\pi^-\pi^0$ or $\bar{K}^0 n\pi^-\pi^+$ events were found.

After correcting for the neutral decay of the $\bar{K}^0$ and its escape probability, we find that these 133 events correspond to 432 $\bar{K}^0 n$ and 106 $\bar{K}^0 n\pi^0$ events. The angular distribution of the $\bar{K}^0 n$ events (including the correction due to escape proability) is shown in Fig. 5.

In the group of events involving the decay of a Λ (about 200 events), it is much more difficult to separate the individual reactions. First, a larger number of reactions can produce a Λ zero-prong event that can produce a $\bar{K}^0$ event. Secondly, the kinetic energy of the Λ in the $K^- p$ c.m. system does not determine uniquely the reaction responsible. Thirdly, in general, the momentum of the Λ is not known as accurately as is the momentum of the $\bar{K}^0$ after they are fitted to their decay.

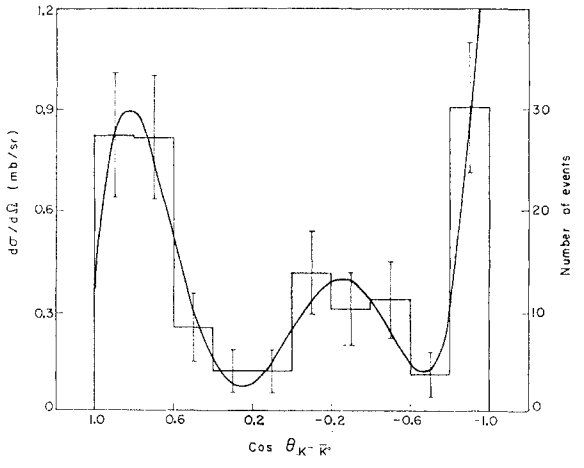

FIG. 5. Angular distribution of the $\bar{K}^0 n$ events in the $K^- p$ c.m. system. The curve shown in the figure represents a least-squares fit of the data to the power series in $\cos\theta$ up to $\cos^5\theta$.

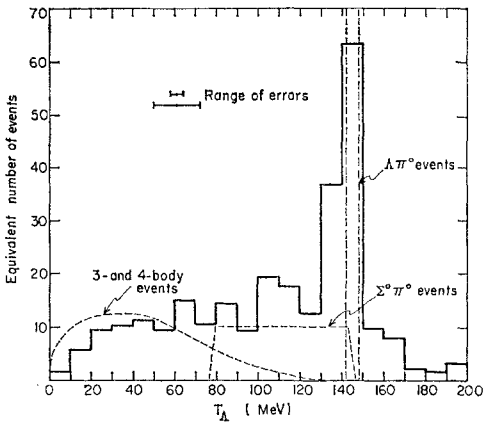

FIG. 6. Kinetic-energy spectrum of Λ in the $K^- p$ c.m. system. The dashed curves are the spectra of $\Lambda\pi^0$, $\Sigma^0\pi^0$, and many-body reactions normalized to the observed cross sections. The $\Lambda\pi^0$ peak should be about three times as high as indicated. Only the spread due to the finite beam width of ± 20 MeV/c is folded in. The curve for many-body events was drawn to reproduce the Λ spectrum of V^0 two-prong events. The errors indicated are median values for the better-measured and worse-measured halves of events.

Some measure of these difficulties is illustrated in Fig. 6, which shows the kinetic energy spectrum of the Λ (including the correction due to escape probability) in the $K^- p$ c.m. system for the Λ zero-prong events. The Lorentz transformation was performed using the nominal beam momentum; the spread in the beam momentum corresponds to a spread on the average of ± 3 MeV in T_Λ. The dashed curves show the spectra of $\Lambda\pi^0$, $\Sigma^0\pi^0$, and many-body events normalized to the observed cross sections; the procedure used in obtaining these cross sections will be discussed next.

We know that the $\Lambda\pi^0$ spectrum is a line and the $\Sigma^0\pi^0$ spectrum must be flat between its two limits. To obtain the Λ spectrum for the many-body events, we assume that the Λ spectrum for the many-body events is the same as the Λ spectrum for the Λ two-prong events. This assumption may be incorrect, because different isotopic spin combinations would be involved in the two classes of reactions. However, since there seems to be no evidence in favor of a sizable π-π interaction in the Λ two-prong events (this is the effect that would alter most drastically the two spectra), it seems plausible to assume *a priori* that the Λ spectrum for three- and four-body Λ zero-prong events is similar to the Λ spectrum in the Λ two-prong events.

To determine the total and differential cross sections for the $\Sigma^0\pi^0$ events, we used the Λ hyperons that were well outside of the $\Lambda\pi^0$ peak. Thus we limited ourselves to the events in which the Λ had a kinetic energy between 78.2 and 122.7 MeV (this represents the lower two-thirds of the $\Sigma^0\pi^0$ spectrum). In imposing this restriction, we are rejecting events in which the cosine of the decay angle $\theta_{\Sigma\Lambda}$ of the Σ^0 in its rest system is greater than 0.33.

This restriction in no way biases our sample, because the Σ^0 decay is completely isotropic and is uncorrelated with the production process.

We assume that the sample of events selected in this manner contains only $\Sigma^0\pi^0$ along with three- and four-body events. The probability that an actual $\Lambda\pi^0$ event would yield a T_Λ less than 122.7 MeV is very small; we estimate that no more than one or two $\Lambda\pi^0$ events are included in this sample.

By summing the weights of the Λ zero-prong events with $T_\Lambda < 78.2$ MeV and assuming that the Λ spectrum for the many-body events is the same as for the Λ two-prong events, we can calculate the total number of Λ many-body events and also the number of Λ many-body events in the region where T_Λ is from 78.2 to 122.7 MeV. Using this information on the Λ many-body events, we were able to estimate the total number of $\Sigma^0\pi^0$ events.

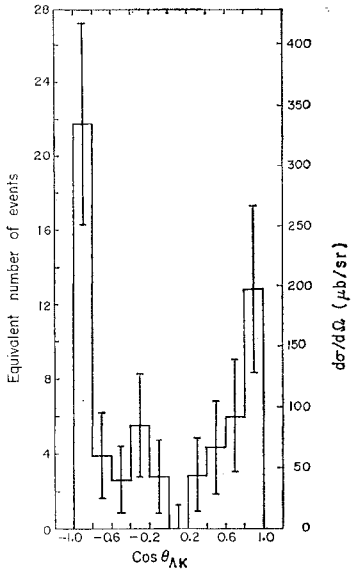

FIG. 7. Angular distribution of Λ in the K^-p c.m. system. Included are events with 78.2 MeV $< T_\Lambda <$ 122.7 MeV, i.e., most likely $\Sigma^0\pi^0$ events. The right-hand scale is based on the total $\Sigma^0\pi^0$ cross sections of 1.2 mb.

The angular distribution of the secondary Λ for events with T_Λ from 78.2 to 122.7 MeV is shown in Fig. 7. We estimate that 2/3 of these Λ hyperons are produced in the reaction $K^-+p \rightarrow \Sigma^0+\pi^0$ with Σ^0 decaying into $\Lambda^0+\gamma$. Fortunately, at this energy the angular distribution of these Λ^0 hyperons reproduces almost completely the angular distribution of the Σ^0 hyperons; the difference is certainly insignificant in comparison to the statistical uncertainties involved in the angular distribution. The angular distribution of the events with $T_\Lambda < 78.2$ MeV is shown in Fig. 8. It is reasonable to assume that the angular distribution for the three- and four-body reactions does not change drastically with the increasing energy of the hyperon; thus the histogram in Fig. 8 might be a reasonably good estimate of the many-body contamination in Fig. 7. No subtraction of background was attempted because of the many uncertainties involved.

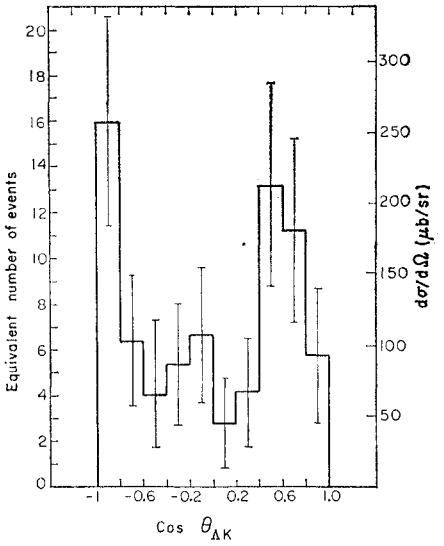

FIG. 8. Angular distribution of Λ in the K^-p c.m. system. Included events have $T_\Lambda < 78.2$ MeV, i.e. most likely three- and four-body events. The right-hand scale is based on the total three- and four-body cross section of 1.5 mb.

Figure 9 shows the angular distribution of all events with $\chi^2 < 2.0$ for the $\Lambda\pi^0$ interpretation. This histogram is probably biased in favor of forward Λ hyperons (and thus should not be taken too literally), since the secondary Λ from a forward Σ^0 hyperon will in general have a larger error on its kinetic energy than a slow Λ (from a backward Σ^0). Thus events with forward Σ^0 are more likely to give a low χ^2 for the $\Lambda\pi^0$ interpretation than are backward Σ^0 events.

The polarization for the three classes of events ($\Lambda\pi^0$, $\Sigma^0\pi^0$, and three- and four-body events) was calculated using all the events found. As previously mentioned, our

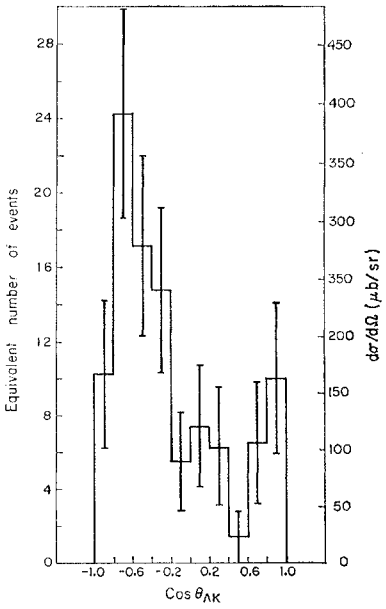

FIG. 9. Angular distribution of Λ in K^-p c.m. system. Included events give $\chi^2 < 2.0$ to the $K^-+p \rightarrow \Lambda+\pi^0$ hypothesis. The right-hand scale is based on the total $\Lambda\pi^0$ cross section. The number of forward-produced Λ particles is probably overestimated (see text for the discussion of this point).

scanning biases would not tend to favor either the "up" or "down" events. In Table I, the polarization results are given for these reactions. The same sign convention is used as for the $\Sigma^{\pm}\pi^{\mp}$ reactions, except that now $\mathbf{P}_Y$ refers always to the momentum of the Λ.

C. Two-Prong Events

The analysis of two-prong event is complicated because of the relatively large number of reactions that can produce this configuration. At our momentum of 1.15 BeV/c, the following reactions can appear as two-prong events (Fig. 3) in a hydrogen bubble chamber:

$$K^-+p \rightarrow K^-+p \tag{8}$$
$$\rightarrow K^-+p+\pi^0 \tag{9}$$
$$\rightarrow \pi^-+p+\bar{K}^0 \tag{10}$$
$$\rightarrow K^-+\pi^++n \tag{11}$$
$$\rightarrow \pi^-+\pi^++\begin{pmatrix}\Lambda\\ \Sigma^0\end{pmatrix} \tag{12}$$
$$\rightarrow \pi^-+\pi^++\begin{pmatrix}\Lambda\\ \Sigma^0\end{pmatrix}+\pi^0 \tag{13}$$
$$\rightarrow K^-+N+2\pi, \tag{14}$$
$$\pi^-+p \rightarrow \pi^-+p \tag{15}$$
$$\rightarrow \pi^-+p+\pi^0 \tag{16}$$
$$\rightarrow \pi^-+\pi^++n \tag{17}$$
$$N+3\pi. \tag{18}$$

Unfortunately, at this momentum, if an event fits a given inelastic K^- hypothesis, it will usually fit also the corresponding π^- hypothesis. That is, a $K^-+p \rightarrow K^-+p+\pi^0$ reaction will ordinarily give a satisfactory χ^2 value for the $\pi^-+p \rightarrow \pi^-+p+\pi^0$ hypothesis. Moreover, the ambiguity cannot be resolved by inspecting the ionization of the outgoing particles, since the momentum of the negative track is usually in the region where both π^- and K^- are minimum-ionizing. To reduce this difficulty, we decided to analyze the two-prong events only in the film sample in which the ratio of incident π^- to K^- particles was 0.08 ± 0.11. This film sample, representing approximately 40% of our data, contained about 900 two-prong events.

We fitted each of these events to interpretations (8) through (12) and (15) through (17). The remaining reactions had two missing neutral tracks and, therefore, could not be fitted. Since the fits to the elastic hypothesis (8) and (15) normally have four constraining equations, it is highly improbable that an inelastic event would fit an elastic interpretation. First, the two outgoing tracks would have to be coplanar with the incident track. This is very unlikely, because coplanarity can be accurately checked, since the directions of the particles can be measured very precisely in a bubble chamber (typical azimuth and dip errors are ±0.2 degrees). In addition to this, the event would have to satisfy the other three constraining equations. Accordingly, the events were divided into two groups, elastic and inelastic, depending on whether they did or did not fit an elastic interpretation. Using this method to classify our reactions, we found approximately 600 elastic and 300 inelastic events.

For 29 of the 300 events that were classified as inelastic events, the momentum of one of the outgoing tracks was unmeasurable. These are primarily short tracks from events that occurred near one of the edges of the bubble-chamber picture. Since these 29 events could not be fitted and were not biased with respect to the reaction that produced them, they were treated as unmeasurable inelastic events. In addition, we had 12 events that were unmeasurable because of poor film quality or difficulties with the bubble chamber. All of the cross sections for the two-prong events have been corrected to account for these two groups of unmeasurable events.

1. Elastic Events

The scanning efficiency for the elastic events depends upon the scattering angle and the orientation of the plane of the event. For scattering angles larger than 5 deg (lab), our detection efficiency is nearly 100% regardless of the orientation of the scattering plane. Below 5 deg the detection efficiency has strong dependence on both the scattering angle and the plane of the event. Therefore we applied a cutoff angle and analyzed only the events with a scattering angle in the lab system greater than 10 deg. This corresponds to a recoil proton with a 2.5-cm range and to a $\cos\theta$ of 0.95 in the c.m. system.

The elimination of the events with $\cos\theta>0.95$ left us with 511 events which fitted the Kp elastic hypothesis and 44 events which fitted only the πp interpretation. Most of these 511 events also fitted the π^- interpretation. Thus, to determine the numer of Kp events we had to estimate the number of πp events that fitted the Kp interpretation.

To obtain an estimate of the total number of π^- elastic events, we examined the elastic scatters that had a $\cos\theta$ less than -0.3, where θ is the angle, in the Kp (or πp) c.m. system, between the incident and final directions of the negative particle. In this cosine interval, the kinematics of the two reactions are sufficiently distinct so that none of these events fitted both π^- and K^- elastic interpretations. Nine of the 75 events with $\cos\theta<-0.3$ fitted the πp hypothesis.

Using the fitted data on the elastic two-prong events, we found that the lower limit for the momentum spectrum of the π^- contamination was approximately 700 MeV/c. The upper limit was about 1150 MeV/c, since our beam would not accept a particle with a momentum larger than this. Fortunately, the angular distribution for πp elastic scattering has been measured at 680,[9]

TABLE II. Summary of data for elastic events.[a]

Total number of observed elastic scatters	555
Number of observed elastic scatters that fitted the K^-p hypothesis	511
Number of observed elastic scatters that fitted only the π^-p hypothesis	44
Estimated number of low energy K^-p elastic scatters that fitted only the π^-p interpretation	11 ± 5
Estimated number of π^-p elastic scatters	38 ± 14
Estimated number of π^-p scatters that fitted the K^-p elastic-scattering interpretation	5 ± 15

[a] Events with $\cos\theta > 0.95$ are not included in this table.

730,[9,10] 780,[10] 850,[9] 880,[10] 939,[11] 1030,[9] 1045,[12] 1130,[13] and 1150 MeV/c.[9] Using these angular distributions, we estimated the value of R, the ratio of the number of events with $\cos\theta < -0.3$ to the number with $\cos\theta < 0.95$, for each of the nine momenta at which the πp two-prong events occurred. This ratio varies quite slowly in this momentum interval (from 0.15 to 0.30). Using these ratios, we estimated that there were 38 ± 14 πp elastic events with $\cos\theta < 0.95$.

Of the two-prong elastic events, 44 fitted only the πp interpretation. However, some of these 44 are Kp elastic reactions which failed to fit the Kp elastic hypothesis because they were produced by a low-momentum incident K meson. (As mentioned earlier, the measured momentum of the incident particle was averaged with 1150 ± 20 MeV/c for the K^- but not the π^- interpretation.) From the study of our τ decays, we estimated that in about 2.5% of the beam tracks the momentum of the K^- meson would be low enough that the event would not fit a K^-p elastic interpretation when the incident track is beam-averaged. Thus approximately 11 ± 5 of these 44 events are actually low-energy K^-p elastic scatters.

Table II summarizes the breakdown of the elastic events. Since we estimate that only 5 ± 15 of the events that fitted the K^-p hypothesis are actually π^-p scatters, the π^- contamination in this sample is neglected in the discussion which follows. Figure 10 shows the angular distribution for the events which fitted the K^-p elastic-scattering interpretation.

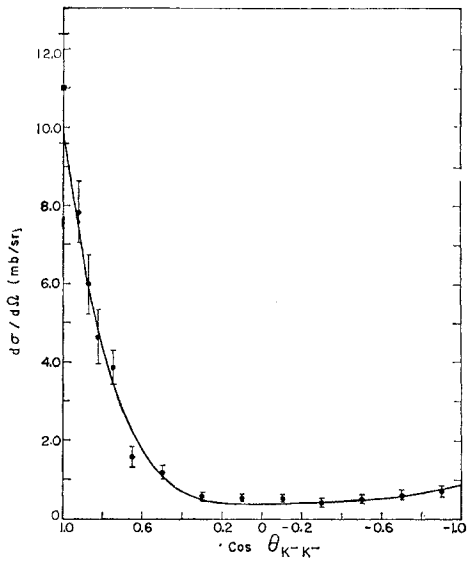

FIG. 10. Angular distribution for the $K^-+p \to K^-+p$ reaction in the c.m. system. A cutoff on the experimental data was imposed at $\cos\theta=0.95$ (see text). The point at $\cos\theta=1.0$ represents the square of the imaginary part of the forward-scattering amplitude; it was calculated by using the optical theorem. The curve represents a least-squares fit of the data to the power series in $\cos\theta$ up to $\cos^5\theta$.

2. Inelastic Two-Prong Events

Analysis of the inelastic events is more difficult than analysis of the elastic reactions, since more interpretations are possible, and the fits to these interpretations have only one independent constraining equation. Since an inelastic event has only one constraint, it will usually fit more than one interpretation. However, more information can be obtained about an event by looking at the ionization of the outgoing tracks. If the momentum of the positive track is less than 800 MeV/c, we can ordinarily distinguish a π^+ meson from a proton by the ionization of the track. For a negative track with momentum up to approximately 400 MeV/c, we can usually distinguish a π^- from a K^- meson. Unfortunately, even after inclusion of the information obtained from the ionization of the outgoing tracks, we still cannot decide upon an unambiguous interpretation for most of the inelastic events. The addition of the ionization data, however, does enable us to separate the inelastic two-prong events into two groups, group P and group π^+, depending on whether the positive track is a proton (group P) or a π^+ meson (group π^+).

To obtain the cross section for a given reaction, we must be able to estimate the number of events due to the other reactions in the same group. Accordingly, the following method was used to determine the cross sections for the final states $K^-p\pi^0$ and $K^-n\pi^+$:

1. We removed from group P the events which do not give a satisfactory fit to either hypothesis (9) or (16). From group π^+ we removed the events for which neither hypothesis (11) nor (17) yield a satisfactory fit.

2. In addition to producing inelastic two-prong events, reactions (10), (12), and (13) also produce V^0 two-prong events. These V^0 two-prong events are much less difficult to analyze than the inelastic two-prong events, and they have been studied in detail.[2,8] The data on these V^0 two-prong events were used to determine the number

[9] C. Wood, T. Devlin, J. Helland, M. Longo, B. Moyer, and V. Perez-Mendez, Phys. Rev. Letters **6**, 481 (1961).
[10] John I. Shonle, University of California Lawrence Radiation Laboratory Report, UCRL-9362, thesis, 1960 (unpublished).
[11] Lee Baggett, Jr., University of California Lawrence Radiation Laboratory Report UCRL-8302, M.S. thesis, 1958 (unpublished).
[12] S. Bergia, L. Bertocchi, V. Borelli, G. Broutti, L. Chersovani, L. Lavatelli, A. Minguzzi-Ranzi, R. Fosi, P. Waloschek, and V. Zoboli, Nuovo cimento **15**, 551 (1960).
[13] I. Derado and N. Schmitz, Phys. Rev. **118**, 309 (1960).

of events remaining in group P due to reaction (10) and the number remaining in group π^+ due to reactions (12) and (13).

3. The number of π^-p elastic scatters were used to estimate the number of events in group P due to reaction (16) and the number in group π^+ due to reaction (17).

4. Finally, we estimated the number of events in the two groups due to reactions other than (9) through (13) and (15) through (17).

Step 2 was performed by taking our V^0 two-prong events, disregarding the data on the V^0, and fitting the event to all the two-prong interpretations [reactions (8) through (13) and (15) through (17)]. For each V^0 two-prong event that gives a satisfactory fit to one of the reactions (9), (10), (16), or (17) there will be $C(1-p)/p$ two-prong events in the π^+ or P group due to reactions (11) through (13). Here, p is the probability that a given event would be detected, which takes account both of the neutral decay mode of the V^0's and of the escape probability; C is the ratio of the number of K^- decays in the reduced film sample (π^- contamination $=0.08\pm0.11\%$) to the total number of K^- decays, i.e., C corrects for the fact that these V^0 two-prong events were taken from the whole film sample, whereas the two-prong events were not. By this method, we concluded that 47 ± 7 of the events in group P were due to reaction (11) and 54 ± 8 in group π^+ were due to reactions (12) and (13).

To estimate the number of $\pi^-+p\rightarrow\pi^-+p+\pi^0$ events in group P, and of $\pi^-+p\rightarrow\pi^-+\pi^++n$ in groups π^+ (step 3), we used the number of π^-p elastic scatters obtained in the analysis of the two-prong elastic events. The cross sections for $\pi^-+p\rightarrow\pi^-+p+\pi^0$ and $\pi^-+p\rightarrow\pi^-+\pi^++n$ events have been measured at only two points in the momentum spectrum of our incident π^- mesons. Cross sections for π^- elastic scattering and for the above two reactions have been measured by Baggett[11] at 0.939 BeV/c and by Derado and Schmitz[13] at 1.13 BeV/c. The following ratios were calculated from their results:

$$V_1=\frac{(\pi^-p\rightarrow\pi^-p\pi^0)}{(\pi^-p\rightarrow\pi^-p)}=0.30\pm0.04 \text{ at } 0.939 \text{ BeV}/c,$$
$$=0.24\pm0.06 \text{ at } 1.0 \text{ BeV}/c;$$

$$V_2=\frac{(\pi^-p\rightarrow\pi^-\pi^+n)}{(\pi^-p\rightarrow\pi^-p)}=0.76\pm0.06 \text{ at } 0.939 \text{ BeV}/c,$$
$$=0.47\pm0.11 \text{ at } 1.0 \text{ BeV}/c.$$

Multiplying the value of V_1 and V_2, measured at 0.939 BeV/c, by the total number of elastic πp events, we obtained 11 ± 5 and 22 ± 9 as the number of $\pi^-p\pi^0$ and $\pi^-\pi^+n$ events, respectively. Using instead V_1 and V_2 measured at 1.13 BeV/c, we obtained 14 ± 5 $\pi^-p\pi^0$ and 35 ± 12 $\pi^-\pi^+n$ events. Since the two estimates for the reactions are approximately within each other's errors, we calculated the average of them and used these averages (12 ± 5 and 27 ± 8) for the number of events in groups P and π^+ due to the reactions $\pi^-p\rightarrow\pi^-p\pi^0$ and $\pi^-p\rightarrow\pi^-\pi^+n$. Since most of our πp events are in the momentum interval from 850 to 1050 MeV/c, these averages shold represent a reasonably accurate estimate for the number of π^- inelastic events.

TABLE III. Summary of inelastic two-prong data.

	Group P	Group π^+
Number of observed events in each group	100 ± 10	160 ± 13
Number of observed events in group P (group π^+) that fitted either reaction (9) or (16) [(11) or (17)]	94 ± 10	154 ± 13
Number of observed events in group P (group π^+) that fitted reaction (9) (11)	47 ± 7	76 ± 9
Estimated number of events in group P (group π^+) due to reaction (12) [(13) and (14)]	47 ± 7	54 ± 8
Estimated number of $\pi\pi N$ events	13 ± 5	27 ± 8
Estimated number of non-two-prong events in groups P and π^+	4 ± 2	8 ± 3
Estimated number of $K^-p\pi^0(K^-\pi^+n)$ events in group P (group π^+)	30 ± 13	65 ± 15

Finally (step 4), we had to consider whether there was any significant contamination in groups P and π^+ due to special configurations of other reactions. Possible candidates are:

(a) $\Sigma^\pm\pi^\mp(\pi^0)$ with a short $\Sigma^\pm$;
(b) $\Sigma^\pm\pi^\mp(\pi^0)$ with the $\Sigma^\pm$ decaying outside the chamber;
(c) $\Sigma^\pm\pi^\mp(\pi^0)$ with a small-angle Σ decay;
(d) $\Lambda+n\pi^0$ (for $n\geqslant1$). with a very short Λ;
(e) $\Sigma^0+n\pi^0$ (for $n\geqslant1$) with a very short Λ;
(f) $\bar{K}^0n(\pi^0)$ with a very short $\bar{K}^0$.

These six categories represent special cases of reactions that we have analyzed previously (reference 4 and Sec. II A, B). Using approximately the same method as in step 2, we estimated the number of two-prong events in groups P and π^+ due to reactions (a) through (f).

The number of reactions of type (14) is probably negligible, since in the entire film sample we have only one example of the reaction

$$K^-p\rightarrow K^-p\pi^+\pi^-$$

and no examples, among our V^0 two-prong events, of the reaction[3]

$$K^-+p\rightarrow\bar{K}^0p\pi^-\pi^+ \quad \text{or} \quad K^-p\rightarrow\bar{K}^0n\pi^+\pi^-.$$

Table III contains a summary of the inelastic two-prong data. In group π^+, 76 events gave a satisfactory χ^2 to the $K^-\pi^+n$ interpretation. From the above analysis we estimate that 65 ± 15 of these are actual examples of the $K^-\pi^+n$ reaction. Similarly, of the 47 events in group P that fitted the $K^-p\pi^0$ hypothesis, 30 ± 13 are estimated to be genuine $K^-p\pi^0$ events. Thus, these 76 and 47 events form a reasonably pure sample for the $K^-\pi^+n$ and $K^-p\pi^0$ reactions, respectively.

TABLE IV. $\Sigma\pi$ angular distributions fitted to $f(\theta)=\Sigma_n A_n \cos^n\theta$.

Event type	Order of fit	A_0	A_1	A_2	A_3	A_4	A_5	A_6	Degrees of freedom	χ^2	Probability of exceeding this χ^2 (%)
$\Sigma^-\pi^+$	3	0.24±0.08	−0.19±0.29	1.14±0.28	3.00±0.56				6	7.4	29
	4	0.27±0.10	−0.18±0.28	0.57±0.88	0.26±0.54	0.72±1.17			5	7.1	22
	5	0.28±0.09	−1.08±0.39	0.80±0.85	5.99±2.27	0.48±1.10	−6.21±2.38		4	0.3	99
	6	0.29±0.11	−1.08±0.45	0.62±1.92	6.05±2.30	1.18±6.55	−6.26±2.41	6.05±5.60	3	0.25	96
$\Sigma^+\pi^-$	3	0.12±0.09	−0.74±0.37	1.32±0.35	1.01±0.71				6	8.4	21
	4	0.15±0.10	−0.76±0.38	0.78±1.10	0.99±0.73	0.82±1.56			5	8.1	15
	5	0.17±0.09	−1.54±0.49	1.16±1.01	6.85±2.61	0.23±1.40	−6.66±2.82		4	5.5	24
	6	0.08±0.09	−1.41±0.43	3.08±1.81	5.95±2.24	−7.95±6.19	−5.71±2.41	7.10±5.34	3	0.7	87
Combined $\Sigma^+\pi^-$ and $\Sigma^-\pi^+$	3	0.18±0.06	−0.51±0.22	1.24±0.22	0.81±0.44				6	15.5	2
	4	0.21±0.07	−0.56±0.22	0.62±0.70	0.77±0.44	0.94±0.97			5	14.6	1
	5	0.23±0.06	−1.32±0.30	0.92±0.62	6.50±1.67	0.38±0.87	−6.48±1.81		4	1.8	77
	6	0.20±0.06	−1.31±0.30	1.75±1.20	6.26±1.60	−3.09±4.22	−6.19±1.73	3.06±3.68	3	1.1	78

IV. RESULTS

A. $\Sigma\pi$ and $\Lambda\pi$ Events

The angular distributions for the reactions $K^-+p\rightarrow\Sigma^\pm+\pi^\mp$ are shown in Fig. 4. We fitted these distributions, using the method of least squares, to a power series in $\cos\theta$. Goodwin has described the method and the IBM 650 program that were used to perform the fits.[14] Table IV shows the results of these least-squares fits. We did not attempt to fit the $\Sigma^0\pi^0$ angular distribution, shown in Fig. 7, because of the large errors that are inherent in this distribution.

Because of limited statistics on these reactions, one cannot estimate which partial waves participate. However, one can combine the data on the $\Sigma^+\pi^-$ and $\Sigma^-\pi^+$ reactions to obtain higher statistical significance. This amounts to looking only at the intensities in the $T=0$ and $T=1$ states and neglecting the possible cross terms which are present in the individual charge states. A fit to a power series in $\cos\theta$ shows that the $\cos^5\theta$ term is both necessary and sufficient to adequately represent the data (Fig. 4(c) and Table IV). This implies that at least a mixture of D and F waves in the $j=5/2$ state is present either in $T=0$ or $T=1$ amplitude.

The cross sections for the three $\Sigma\pi$ reactions are given in Table V. These cross sections are equal within statistical errors. The equality of the three $\Sigma\pi$ cross sections and the similarity of their angular distributions (Figs. 4 and 7) suggest that the $\Sigma\pi$ events are produced mainly in the $T=0$ channel. However, because of the large errors on the $\Sigma^0\pi^0$ section and angular distribution, a $T=1$ amplitude equal to about 80% of the $T=0$ amplitude cannot be excluded (see also the data on polarization, below). A $T=1$ amplitude of this magnitude would require that the two I-spin amplitudes be orthogonal for the $\Sigma^+\pi^-$ and $\Sigma^-\pi^+$ cross sections to be equal. Furthermore, the similarity of the charged and neutral $\Sigma\pi$ angular distributions would have to be a coincidence. It thus seems likely that the $\Sigma\pi$ production at this energy is dominated by the $T=0$ amplitude.

In our analysis of the $\Sigma^+\pi^-$ reactions, we found that the Σ^+ hyperons from this reaction are very strongly polarized. For the $\Sigma^+\pi^-$ events that decayed via the protonic mode, $\alpha\bar{P}$ was found to be -1.02 ± 0.23. In calculating this value, we imposed no cutoff on the production angle. Thus the polarization of the Σ^+ must persist up to very small production angles.

If the three $\Sigma\pi$ reactions are produced mainly through the $T=0$ channel, then the Σ^0 and Σ^- hyperons should also be very highly polarized. Unfortunately, the Σ^- polarization cannot be determined, since α for the Σ^- decay is very small. The Σ^0 polarization, however, can be studied by looking at the up-down asymmetry of the Λ produced in the Σ^0 decay.

Unfortunately, there are several difficulties in deter-

TABLE V. Summary of K^-p cross sections at 1.15 BeV/c.

Final state	Number of events	Cross section (mb)
K^-+p	511	18.3 ±1.5
$\bar{K}^0+n$	107	5.3 ±0.5
$K^{*-}+p$	21[a]	1.35±0.3
$K^{*0}+n$	28[a]	0.9 ±0.15
$K^-+p+\pi^0$	30[a]	1.0 ±0.3[b]
$K^-+\pi^++n$	65[a]	2.1 ±0.4[b]
$\bar{K}^0+n+\pi^0$	26	1.3 ±0.3[b]
$\bar{K}^0+p+\pi^-$	48	2.0 ±0.3[b]
$\Sigma^-+\pi^+$	87	1.4 ±0.2
$\Sigma^++\pi^-$	84	1.3 ±0.2
$\Sigma^0+\pi^0$	50[a]	1.2 ±0.3 (±0.45)[c]
$\Lambda+\pi^0$	90[a]	2.1 ±0.2 (±0.35)[c]
$\Sigma^++\pi^-+\pi^0$	57	1.0 ±0.2 (±0.3)[c]
$\Sigma^-+\pi^++\pi^0$	54	0.8 ±0.2 (±0.3)[c]
$\Sigma^0+\pi^-+\pi^+$	27	1.0 ±0.2 $(_{-0.2+}{}^{0.4})$[c,d]
$\Lambda+\pi^++\pi^-$	141	3.1 ±0.4[c]
$\left.\begin{matrix}\Lambda+x\pi^0\\ \Sigma^0+x\pi^0\end{matrix}\right\}x\geq 2$	65[a]	1.5 ±0.2 (±0.35)[c]
$\Sigma^++\pi^-+\pi^0+\pi^0$	13	0.18±0.06 (±0.12)[c]
$\Sigma^-+\pi^++\pi^0+\pi^0$	9	0.12±0.05 (±0.08)[c]
$\Sigma^++\pi^-+\pi^++\pi^-$	19	0.19±0.06
$\Sigma^-+\pi^++\pi^-+\pi^+$	13	0.12±0.05
$\left.\begin{matrix}\Lambda+\pi^++\pi^-+x\pi^0\\ \Sigma^0+\pi^++\pi^-+x\pi^0\end{matrix}\right\}x\geq 1$	39	1.1 ±0.2[d]

[a] This represents the approximate number of events since the separation was performed on a statistical basis.
[b] The $KN\pi$ cross sections include K^* events.
[c] The first error quoted is purely statistical. The error in parentheses allows for biases and ambiguities in the analysis.
[d] The data for V^0 two-prong reactions come from reference 3.

[14] Lester K. Goodwin, University of California Lawrence Radiation Laboratory Report UCRL-9263, 1960 (unpublished).

TABLE VI. K^-p elastic- and charge-exchange scattering angular distributions fitted to $f(\theta)=\Sigma_n A_n \cos^n\theta$.

Reaction	Order of fit	A_0	A_1	A_2	A_3	A_4	A_5	A_6	A_7	$d\sigma/d\Omega$ at 0 deg (mb/sr)	Degrees of freedom	χ^2	Probability of exceeding this χ^2 (%)
K^-p	3	0.10±0.02	−0.01±0.08	1.35±0.10	1.31±0.16					6.5±0.3	9	33.2	<1
	4	0.15±0.04	−0.19±0.09	0.36±0.28	1.78±0.19	1.53±0.35				8.8±0.7	8	13.5	9
	5	0.16±0.03	−0.01±0.12	0.14±0.25	0.54±0.63	1.85±0.38	1.38±0.70			10.1±1.0	7	9.6	21
	6	0.14±0.03	0.03±0.13	0.50±0.51	0.27±0.70	0.37±1.84	1.66±0.79	1.32±1.65		10.9±1.4	6	9.0	17
	7	0.14±0.03	−0.09±0.19	0.58±0.51	1.84±1.84	−0.53±1.86	−2.91±0.50	1.74±1.68	3.51±3.81	12.2±1.9	5	8.1	15
K^0n	3	0.28±0.09	−0.11±0.32	1.08±0.40	1.01±0.62						6	28.8	<1
	4	0.46±0.12	−0.19±0.33	−1.15±0.93	1.00±0.64	3.29±1.27					5	22.1	<1
	5	0.41±0.09	−1.67±0.44	−0.26±0.75	9.50±2.06	1.92±1.02	−9.21±2.11				4	3.1	55
	6	0.38±0.11	−1.61±0.43	0.54±1.73	9.01±2.12	0.38±5.85	−8.75±2.18	1.28±4.99			3	3.0	40

mining the polarization. Firstly, the chain of decays $\Sigma^0 \to \Lambda+\gamma$, $\Lambda \to p+\pi^-$ washes out the polarization by a factor of three (it also changes the sign of the polarization). Secondly, we do not have a pure sample of $\Sigma^0\pi^0$ events. Approximately 30% of the events in the sample were many-body events. In addition to these two difficulties, the Σ^0 production plane is not precisely known. However, it is approximated quite closely at our energy by the $K^-\Lambda$ plane. For the $\Sigma^0\pi^0$ sample we found a value of 0.25 ± 0.26 for $\alpha\bar{P}$.

Present experimental data indicate $\alpha_\Lambda/\alpha_0 \approx -1$.[15] Thus, if we assume production through a pure $T=0$ channel, we would expect our $\Sigma^0\pi^0$ events to yield $\alpha\bar{P}=-0.34\pm0.08$. Even though at first glance the experimental value disagrees with this prediction, we feel that no strong conclusions can be drawn from these data. We must remember that some 30% of the events included in this sample are many-body events. Even if they were unpolarized, they would reduce the expected value of $\alpha\bar{P}$ to ≈ -0.24. A small polarization of the opposite sign would reduce this value even further. Secondly, the present experimental indications are that $-\alpha_\Lambda \approx \alpha_0 \approx 0.7$ rather than 1. This would mean that the high value of $\alpha\bar{P}$ for $\Sigma^+\pi^-$ events is to a certain extent a statistical fluctuation, but would also reduce the expected value of $\alpha\bar{P}$ for $\Sigma^0\pi^0$ events by another 30%. We feel, therefore, that one cannot say that the polarization data excludes, though it certainly does not support, the hypothesis of production dominantly through the $T=0$ channel.

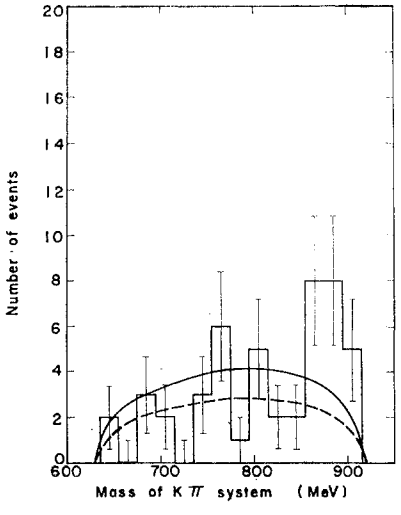

FIG. 11. Mass spectrum of $(K^-\pi^0)$ system from the reaction $K^-+p \to K^-+p+\pi^0$. The solid curve represents the phase-space curve normalized to the total number of events. The dashed curve is normalized to the background (see text).

[15] E. F. Beall, Bruce Cork, D. Keefe, P. G. Murphy, and W. A. Wenzel, Phys. Rev. Letters 8, 75 (1962).

B. $\bar{K}^0n$ and K^-p Events

Figure 5 shows the angular distribution for the reaction

$$K^-+p \to \bar{K}^0+n.$$

We fitted this distribution to a power series in $\cos\theta$ using the same method as for $\Sigma\pi$ reactions. For each of the fits, Table VI lists the values of the coefficients of the polynomials, the χ^2, and the probability that a χ^2 as large as this would have occurred. A $\cos^5\theta$ term seems to be both necessary and sufficient to fit the angular distribution. The curve for the $n=5$ fit, normalized to the total number of events, is plotted with the histogram for the angular distribution in Fig. 5. The cross section for the reaction $K^-+p \to \bar{K}^0+n$ at this energy is 5.3 ± 0.5 mb.

Figure 10 shows the c.m. angular distribution for the $K^-+p \to K^-+p$ reaction. This distribution was also fitted to a power series in $\cos\theta$. The order of the fit, the values of the coefficients of the polynomials, the χ^2, the probability that a χ^2 as large as this would have occurred, and $d\sigma/d\Omega$ at 0 deg are given in Table VI for each of the fits. Here again, $n=5$ is probably necessary to fit the angular distribution. The curve shown in Fig. 10 represents the $n=5$ fit. The point at $\cos\theta=1.0$ (11.0 ± 1.0 mb/sr) represents the square of the imaginary part of the forward-scattering amplitude. This was calculated from the total cross section at this energy (see end of Sec. IV) by using the optical theorem.

To obtain the total number of K^-p elastic scatters, we integrated the fitted curve ($n=5$) between from $\cos\theta=-1.0$ to $\cos\theta=1.0$ and made a small correction for the unmeasurable events. The K^-p elastic-scattering cross section is 18.3 ± 1.5 mb.

C. $KN\pi$ Events

The analysis of our $\bar{K}^0p\pi^-$ events, with V^0 two-prong configuration, showed the existence of a $K\pi$ resonance, called K^*.[3] The mass of this resonance was found to be 885±3 MeV with a full width, after unfolding experimental errors, of 16 MeV. This corresponds to a lifetime of approximately 4×10^{-23} sec. The K^* resonance should display itself in our $K^-p\pi^0$, $K^-\pi^+n$, and $\bar{K}^0n\pi^0$ events. We would expect some of the $KN\pi$ reactions to have been produced by the following two-step processes:

$$K^-+p\rightarrow K^{*-}+p,\quad K^{*-}\rightarrow K^-+\pi^0,$$
$$\rightarrow \bar{K}^{*0}+n,\quad \bar{K}^{*0}\rightarrow K^-+\pi^+,$$
$$\rightarrow \bar{K}^0+\pi^0.$$

The characteristic feature of the K^* reaction is that the nucleon has a fixed kinetic energy of 20±4 MeV in the K^-p c.m. system.

The distributions of the $K\pi$ masses for the $K^-p\pi^0$ and $K^-\pi^+n$ reactions are shown in Figs. 11 and 12. The solid curves in those figures represent the mass distribution predicted by phase space and normalized to the total number of events. The peak in the mass distributions in the two figures at 885 MeV indicates the presence of K^* events, in both of these reactions. The dashed phase-space curves in the two figures are normalized in the interval $M_{K\pi}<835$ MeV and thus represent the three-body background.

To determine the number of K^* events, we took the number of events in the mass interval 885±30 MeV (the error on the $K\pi$ mass ranges from 10 to 30 MeV) and, using the dashed curves, subtracted the number of events due to background. The result is 14±4 $K^{*-}\rightarrow K^-+\pi^0$ and 19±5 $K^{*0}\rightarrow K^-+\pi^+$ events. These numbers correspond to cross sections of 0.48±0.14 mb and 0.64±0.17 mb, respectively (including corrections for unmeasurable events).

The isotopic spin of the K^* can be determined from the value of the branching ratio R, where

$$R=(K^{*-}\rightarrow K^-+\pi^0)/(K^{*-}\rightarrow \bar{K}^0+\pi^-).$$

If the isotopic spin of the K^* equals 1/2, R equals 1/2; if the isotopic spin is 3/2, R is 2. In the analysis of our V^0 two-prong events, we found that the cross section for K^{*-} events, in which the K^{*-} decays into $\bar{K}^0+\pi^-$, is 0.9±0.2 mb.[3] Using the cross section for K^{*-} events, in which $K^{*-}\rightarrow K^-+\pi^0$, we obtained a value for R of 0.5±0.2, and we therefore concluded that the isotopic spin of the K^* is 1/2. This agrees with an earlier preliminary anaysis which was also based on these two-prong inelastic events.[3]

Since the $\bar{K}^0n\pi^0$ events cannot be fitted, we could obtain neither the mass spectrum of the $K\pi$ system for this reaction, nor information about the $K^{*0}n$ reaction from the $\bar{K}^0n\pi^0$ events.

The first pion-nucleon resonance (mass=1238 and Q=160 MeV) could also effect these $KN\pi$ reactions. Its presence would be indicated by an excess of events with pion-nucleon mass in the region of 1238 MeV. No such excess is observed, but this is a rather wide resonance and would therefore be difficult to detect because of the background events and our limited statistics.

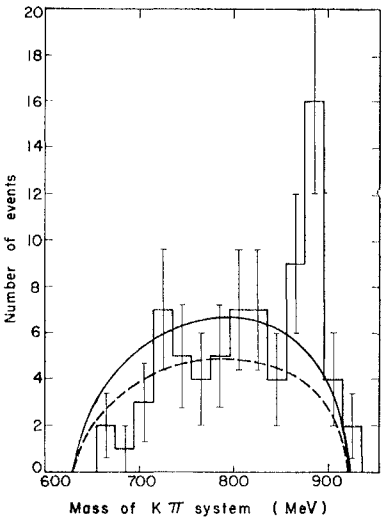

FIG. 12. Mass spectrum of $(K^-\pi^+)$ system from the reaction $K^-+p\rightarrow K^-+\pi^++n$. The solid curve represents the phase-space curve normalized to the total number of events. The dashed curve is normalized to the background.

In reference 3, which discussed the $K^-+p\rightarrow\bar{K}^0+p+\pi^-$ events, evidence was presented for the hypothesis that the K^* has spin less than two. This evidence was based on the assumption that the K^*N system is in a state of zero-orbital angular momentum. There are two justifications for this assumption: One is that the energy region under study (1.15 BeV/c) is only 35 MeV above the K^*N threshold; the other is that the K^*N angular distribution is consistent with isotropy. If the assumption of S-wave production for the K^*N system is valid, the following inequalities involving $\langle\cos^2\theta\rangle_{\rm av}$ can be derived (see reference 3 for the method):

$$\langle\cos^2\theta\rangle_{\rm av}=0.33 \quad \text{for} \quad K^* \text{ spin}=0,$$
$$0.20<\langle\cos^2\theta\rangle_{\rm av}<0.60 \quad \text{for} \quad K^* \text{ spin}=1,$$
$$\langle\cos^2\theta\rangle_{\rm av}>0.429 \quad \text{for} \quad K^* \text{ spin}>1.$$

Here θ represents, in the K^* rest system, the angle that the π meson makes with the incident K^- direction. Except for the $S=0$ case, the exact value of $\langle\cos^2\theta\rangle_{\rm av}$ depends on the mixture of $J=S+1/2$ and $J=S-1/2$ states in the K^*N system (where S is the spin of the K^*).

In our $K^-p\pi^0$ and $K^-\pi^+n$ events we had 21 and 29 events, respectively, in the K^* peak; 14±3 of the 21 and 19±3 of the 29 were K^* reactions. The angular distributions of the 21 and 29 events are both consistent with isotropy; this agrees with the hypothesis of an S-state K^*N system. For $\langle\cos^2\theta\rangle_{\rm av}$ we obtained 0.39±0.07 for 21 $K^-p\pi^0$ events, and 0.43±0.05 for 29 $K^-\pi^+n$ events. In reference 3 we had $\langle\cos^2\theta\rangle_{\rm av}$ =0.275±0.05 for 26 $\bar{K}^0p\pi^-$ events (22±2 were K^* events). The value of $\cos^2\theta$ for the $K^-p\pi^0$ events can be averaged with that for the $\bar{K}^0p\pi^-$ events of reference 3, since they are both examples of $K^{*-}p$ reactions. The

result is 0.31 ± 0.04. Thus taking either the $\bar{K}^0p\pi^-$ data alone or averaging it with the $K^-p\pi^0$ data, We find a value for $\cos^2\theta$ which is three standard deviations from the value expected for a K^* with a spin greater than one. Since the mixture of $J=S+1/2$ and $J=S-1/2$ states could be different for the K^{*-} and for the K^{*0}, we cannot average the values of $\langle\cos^2\theta\rangle_{\text{av}}$ obtained from the two reactions unless S equals zero. Averaging the K^{*-} and K^{*0} data yields 0.36 ± 0.3, which is consistent with $S=0$.

From the value of $\langle\cos^2\theta\rangle_{\text{av}}$ for the 26 $\bar{K}^0p\pi^-$ events, we concluded, in reference 3, that the K^* probably does not have a spin greater than one. Unfortunately, from the results for the 21 $K^-p\pi^0$ and the 29 $K^-\pi^+n$ events, we cannot obtain any additional information about the K^* spin. However, the addition of the $K^-p\pi^0$ and $K^-\pi^+n$ data to the $\bar{K}^0$ data does not alter the conclusion that the K^* probably has a spin less than 2.

Using the branching ratios for the K^* $(I=1)$, we calculated the cross sections for $K^-+p\rightarrow K^{*-}+p$ and $K^-+p\rightarrow K^{*0}+n$. These cross sections, including corrections for unmeasurable events, are shown in Table V. The cross sections for $K^-p\pi^0$, $K^-\pi^+n$, and $\bar{K}^0n\pi^0$, including K^* events (and corrections for unmeasurable events) are also given in Table V.

The total K^-p cross section at 1.15 BeV/c was obtained by combining the results of references 2, 3, and 4 with the results of this paper. Its value is 45 ± 2 mb. Table V contains a summary of the different K^-p cross sections at this energy.

ACKNOWLEDGMENTS

This work has been part of an experiment conducted jointly with Professor Luis W. Alvarez, Professor Myron L. Good, and Professor Harold K. Ticho, and Dr. Margaret H. Alston and Dr. Philippe Eberhard.

The authors would like to express their deep appreciation to Professor Luis W. Alvarez for his continual interest, advice, and encouragement. Sincere thanks are due Professor Myron L. Good and Professor Harold K. Ticho for their help, guidance, and suggestions at all stages of this work. The advice of and discussions with Dr. Margaret Alston have been invaluable in the data analysis. The authors have profited greately from many stimulating discussions with Dr. Philippe Eberhard.

The authors would like to express their thanks to Professor Donald H. Miller and Professor Arthur H. Rosenfeld for many enlightening discussions. Dr. Frank Solmitz has always given freely of his time, and his advice during the early part of the experiment has been invaluable.

This experiment would have been impossible without the highly developed digital-computer data-reduction system. Dr. Frank Solmitz, Dr. William Humphrey, and Dr. Ronald Ross have been mainly responsible for the PANG program, and Professor Arthur H. Rosenfeld, Professor James Snyder, and Professor Horace Taft, Dr. Frank Solmitz, and Jon Peter Berge for the KICK system. Dave Johnson deserves special thanks for his help with the EXAMIN system.

The cooperation of the Bevatron crew under the direction of Dr. Edward J. Lofgren, and of the bubble chamber crew under the direction of Donald Gow, Robert Watt, and Glenn Eckman is acknowledged with many thanks.

Finally, special thanks are due to the scanners who participated in this experiment, especially Joseph Waldman and Jon Folkman.

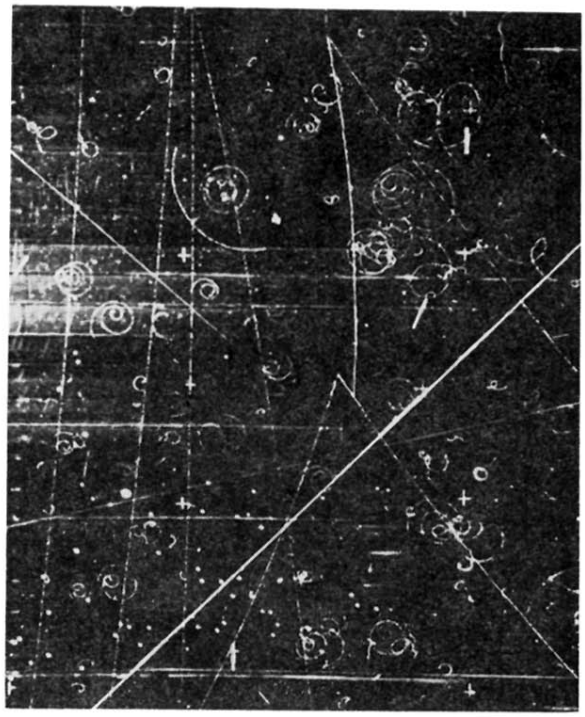

FIG. 2. An example of the reaction:

$$K^- + p \rightarrow K^- + \pi^+ + n,$$
$$K^- + p \rightarrow \Sigma^- + \pi^+$$
$$\searrow$$
$$\pi^- + n.$$